Condition-Invariant Semantic Segmentation

Christos Sakaridis[1], David Bruggemann[1], Fisher Yu[1], and Luc Van Gool[1,2]

[1]ETH Zürich, [2]KU Leuven

Abstract

Adaptation of semantic segmentation networks to different visual conditions from those for which ground-truth annotations are available at training is vital for robust perception in autonomous cars and robots. However, previous work has shown that most feature-level adaptation methods, which employ adversarial training and are validated on synthetic-to-real adaptation, provide marginal gains in normal-to-adverse condition-level adaptation, being outperformed by simple pixel-level adaptation via stylization. Motivated by these findings, we propose to leverage stylization in performing feature-level adaptation by aligning the deep features extracted by the encoder of the network from the original and the stylized view of each input image with a novel feature invariance loss. In this way, we encourage the encoder to extract features that are invariant to the style of the input, allowing the decoder to focus on parsing these features and not on further abstracting from the specific style of the input. We implement our method, named Condition-Invariant Semantic Segmentation (CISS), on the top-performing domain adaptation architecture and demonstrate a significant improvement over previous state-of-the-art methods both on Cityscapes→ACDC and Cityscapes→Dark Zurich adaptation. In particular, CISS is ranked first among all published unsupervised domain adaptation methods on the public ACDC leaderboard. Our method is also shown to generalize well to domains unseen during training, outperforming competing domain adaptation approaches on BDD100K-night and Nighttime Driving. Code is publicly available at https://github.com/SysCV/CISS.

1. Introduction

Unsupervised domain adaptation (UDA) is a primary instance of transfer learning, in which a labeled source set and an unlabeled target set are given at training time and the goal is to optimize performance on the domain of the latter set. There is a large body of literature focusing on UDA for semantic segmentation, which is of high practical importance for central computer vision applications such as autonomous cars and robots, as these systems need to have a dense pixel-level parsing of their surrounding scene, are bound to encounter data from different domains than those annotated for training, and labeling large quantities of data for each new deployment domain is very time- and cost-intensive. The main directions of recent research on this task are adversarial learning for domain alignment [20, 22, 35, 37, 38] and training with pseudolabels [34, 46, 48, 49], with methods primarily focusing on the synthetic-to-real UDA setting [27, 28], i.e., GTA5→Cityscapes and SYNTHIA→Cityscapes. However, the normal-to-adverse Cityscapes→ACDC UDA benchmark introduced in [31] showed that adversarial-learning-based methods, which attempt to align domains at the level of features, struggle with the domain shift from normal to

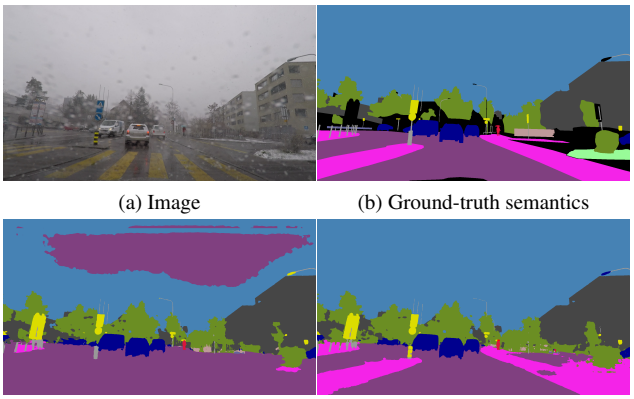

(a) Image (b) Ground-truth semantics

(c) HRDA [13] (d) CISS (ours)

Figure 1. The domain shift from normal to adverse conditions presents challenges to top-performing state-of-the-art domain adaptation methods for semantic segmentation (c) due to the large resulting change in the appearance of classes. We propose a method that encourages invariance of deep segmentation features to visual conditions by comparing features of different views of the same scene under the style of different domains, improving segmentation especially for classes which undergo large shifts.

adverse conditions. By contrast, Fourier domain adaptation (FDA) [43] was shown in [31] to provide significant gains in this normal-to-adverse setting, even with its simple non-learned pixel-level domain alignment.

We recognize that the problem with adversarial approaches is that they discriminate between feature maps that are extracted from *different* scenes, which does not allow to disentangle the difference in the domain from the difference in the scene content. The key idea in this work is to factor out the aforementioned difference in scene content by aligning features that are extracted from two versions of the *same* scene that belong to different domains with a feature invariance loss that penalizes differences between the two feature maps. The intuition is that the encoder of the semantic segmentation network should output features that are invariant to the domain/style of the scene, so that the decoder can subsequently produce identical outputs for the different versions of the scene, as the ground-truth semantics of these versions are also identical. To our knowledge, we are the first to propose this cross-domain internal feature invariance in UDA for semantic segmentation, which hinges on comparing features from different views of the same scene rendered in different domains/styles.

A major challenge in implementing the feature invariance loss is the generation of representative alternative views of input source-domain or target-domain scenes. Instead of relying on learned models which add significant complexity to the overall adaptation architecture or on simple photometric augmentations, we propose to leverage shallow stylization methods, e.g. FDA [43] or simple color transfer [26], to this end. In order to transfer each source-domain image to the style of the target domain, we use the corresponding target-domain image of the training mini-batch and transfer its style to the source-domain image. This allows a light-weight stylization that is simply implemented as part of the data loading in training. The original and stylized source-domain images are then both fed to the segmentation network to compute the feature invariance loss. The converse procedure is followed for each target-domain image of each training mini-batch. As the invariance of features is promoted across views of the scene which are characterized by an identical structure of the objects that are present, we term our method Condition-Invariant Semantic Segmentation (CISS, pronounced *kiss*) to signify that it is tailored for condition-level domain shifts and not shifts involving structural changes of objects, as in the synthetic-to-real setup, where the shape of objects may change across domains. We note that CISS is not specific to the particular stylization it uses and works well with different stylization techniques including [26, 43], as we will review in Sec. 4.

In our experiments, we use the state-of-the-art HRDA [13] architecture and implement CISS on top of it. We show that our feature invariance loss improves significantly upon the straightforward alternative of defining an extra cross-entropy loss on the stylized images. Moreover, the separate feature invariance losses on source and target images are shown to be synergistic, leading to state-of-the-art results both on the Cityscapes→ACDC and Cityscapes→Dark Zurich UDA benchmarks. For ACDC, this regards both the complete test set including night, fog, rain, and snow, and the individual test sets of three conditions, namely night, rain, and snow. Both on the complete test set and on the three aforementioned condition-specific sets, CISS occupies the first place on the respective public ACDC leaderboards among all published UDA methods. Last but not least, we evaluate the CISS model trained for nighttime segmentation on Cityscapes→Dark Zurich in a generalization setting using the BDD100K-night [30, 44] and Nighttime Driving [6] sets and demonstrate the benefit of condition invariance for generalization across diverse nighttime data.

2. Related Work

Unsupervised domain adaptation works often utilize adversarial domain adaptation to align the source and target domains at the level of pixels, intermediate features, or outputs [4, 10, 11, 16, 22, 32, 35, 36, 37, 38, 45]. Other approaches apply self-training with pseudolabels [8, 19, 48, 49] or combine self-training with adversarial adaptation [20]. CyCADA [10] employs a semantic consistency loss with some similarity to our feature invariance loss. This loss optimizes the two generators in the CycleGAN architecture [47] to translate images across the source and target domains in a way which ensures that a *fixed* segmentation network predicts the same labels on the translated versions of the images as in the original images. Importantly, the weights of this fixed segmentation network are not optimized jointly with the rest of the networks that are involved in CyCADA, but a separate segmentation network is rather learned for the target domain, for which no semantic consistency loss is applied. On the contrary, we propose to learn a *single* segmentation network both for the source and the target domain, the intermediate feature representations of which are optimized to be invariant to the input condition. FIFO [18] introduces fog factors, which are intermediate global representations of the characteristics of fog that is (or is not) present in images. These representations are extracted with a separate fog-pass filtering module, which accepts as input intermediate features of the main segmentation network. However, the fog factors—the deviation of which is penalized in [18]—do not always correspond to images with the same content, thus penalizing their deviation does not necessarily enforce condition invariance of the segmentation features. Pixel-level adaptation via explicit transforms from source to target is performed in [15, 43]; we build on the effec-

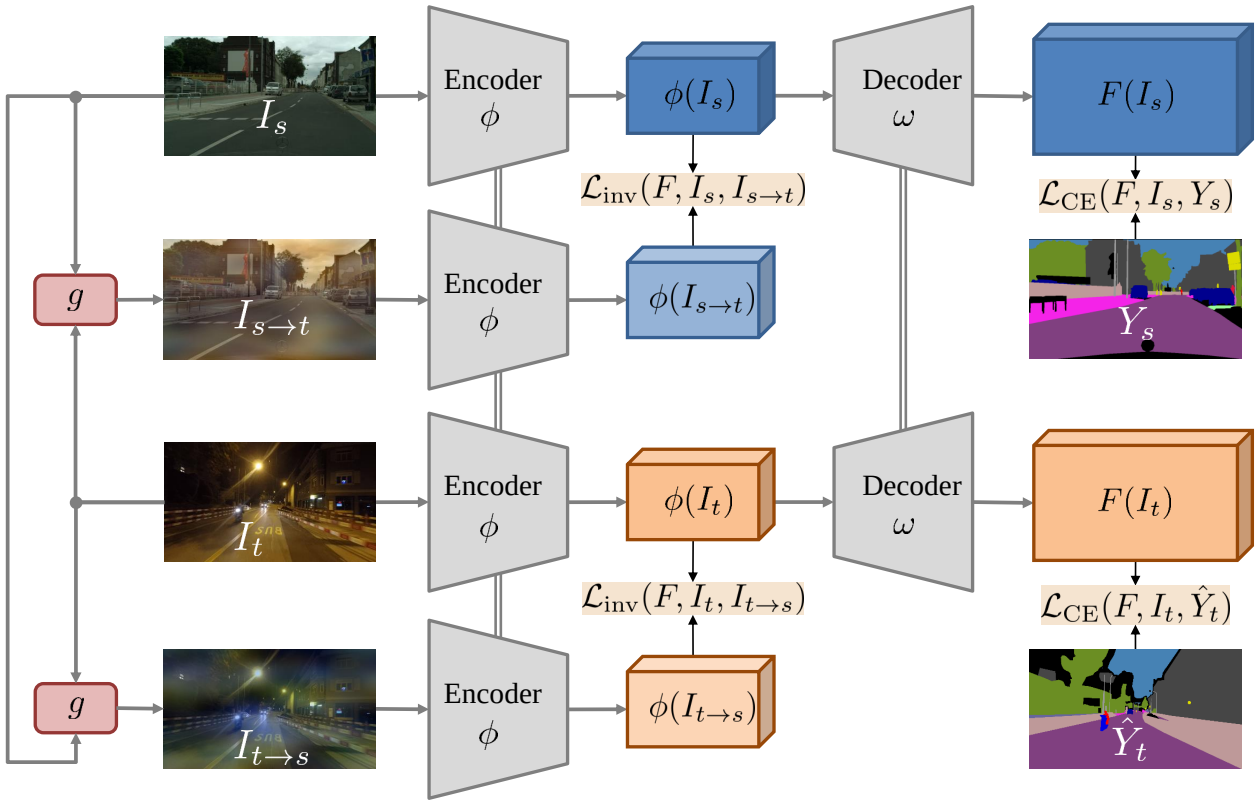

Figure 2. **Overview of our method.** Two instances of a shallow stylization mapping g are fed with the source and target image, I_s and I_t, to produce versions stylized with the converse domain, $I_{s\to t}$ and $I_{t\to s}$. The four images are fed to a shared encoder ϕ, the features of which are used to compute our feature invariance losses. The features of the original source and target images are further fed to a shared decoder ω to compute softmax predictions and respective cross-entropy losses. Double lines indicate shared weights.

tiveness of FDA [43], but only use it as a building block in CISS, which additionally performs feature-level adaptation. Recent works upgrade the architecture and training strategy for UDA [12] and operate at higher resolution [13], delivering significant performance gains; we implement CISS using these architectures and show the additional benefit of condition invariance in this highly competitive setting.

Consistency regularization is used in PixMatch [24] in the context of unsupervised domain adaptation on the target domain, by promoting invariance of the semantic predictions of the segmentation network to various perturbations of the input target image, including changes in the low-frequency part of the Fourier phase of the image and in its style. However, the original target-domain semantic predictions can be false as they constitute pseudolabels and this may impact the learned representations negatively. By contrast, our method promotes invariance of intermediate features, which avoids reliance of consistency regularization on potentially false pseudolabels. The idea of consistent label predictions under input augmentations stems from FixMatch [33], which considers a classification setting; we instead promote consistency at the level of intermediate features in a dense fashion, lifting the need for explicit pseudolabels. Consistency under augmentations has also been found to be important in semi-supervised semantic segmentation [7]; instead of plain augmentations, we employ *stylization* of the input images by exploiting pairs of source and target images that are available at training to obtain better cross-domain image views for promoting invariance. CISS can be viewed as a contrastive learning method, using positive pairs to enforce feature invariance densely at each pixel. Contrastive approaches are also proposed in [1, 14, 17, 41], however, they contrast general pairs of pixels, while we contrast pairs of pixels that depict exactly the same point of the scene, providing stronger positive pairs. A concurrent work [40] with ours implements consistency training with a consistency loss that is similar to our feature invariance loss, however, that work focuses on the domain generalization setting simply using *augmentations* of input images rather than on our UDA setting, for which *stylization* of the images to the style of different domains is essential. Moreover, [40] also applies consistency to the *penultimate* layer of the semantic segmentation network, i.e. at a late stage, and not deeply at the *encoder* outputs, as CISS does. Our strategy is motivated by the intuition that the encoder of the semantic segmentation network should already output features that are invariant to the domain/style of the scene, so that the decoder can subsequently focus on parsing these

features and not on further abstracting from them.

3. CISS

We first provide a basic UDA setup for semantic segmentation, with definitions of inputs, outputs and losses, and then present our UDA method, CISS, which builds on this setup. A visual overview of CISS is presented in Fig. 2.

3.1. A Basic UDA Setup

In modern UDA training pipelines, each training batch contains an equal number B of source and target images. We denote the source images by $\{I_{s,b}\}_{b=1}^{B}$ and the target images by $\{I_{t,b}\}_{b=1}^{B}$. Moreover, the batch contains pixel-level semantic labels of the source images and—in self-training-based methods—of the target images, the latter constituting pseudolabels. We denote these labels by $\{Y_{s,b}\}_{b=1}^{B}$ and $\{\hat{Y}_{t,b}\}_{b=1}^{B}$, respectively. For presenting our method, we assume that the pseudolabels $\{\hat{Y}_{t,b}\}_{b=1}^{B}$ are given, as our focus is not on improving pseudolabel generation, and we defer the details of this generation to Sec. 4.

For the sake of simplicity, we focus on the case where $B = 1$, but our analysis extends straightforwardly to larger B. Dropping the redundant subscripts, the training batch in this case is $(I_s,\, I_t,\, Y_s,\, \hat{Y}_t)$. The basic UDA setup we start from involves training the semantic segmentation network F using both the source-domain and the target-domain sample by applying cross-entropy losses on the outputs of F for the two images. More specifically, if the semantic labels Y are one-hot-encoded in a $C \times H \times W$ tensor, then the cross-entropy loss associated with the softmax output $F(I)$ of the network for I is defined as

$$\mathcal{L}_{\text{CE}}(F, I, Y) = -\frac{1}{CHW} \sum_{c,h,w} Y_{c,h,w} \log \left(F(I)_{c,h,w} \right). \tag{1}$$

Thus, in the basic training setup we start from, the overall loss can be expressed as

$$\mathcal{L}_{\text{basic}} = \mathcal{L}_{\text{CE}}(F, I_s, Y_s) + \mathcal{L}_{\text{CE}}(F, I_t, \hat{Y}_t). \tag{2}$$

This training loss encourages the network to preserve its knowledge on semantics from the source domain with high-quality ground-truth labels while also adapting to the target domain via pseudolabels.

3.2. Pixel-Level Adaptation with Stylized Views

In order to better align the source and target domain, we can translate the input images to the style of the other domain. This is an alignment of the two domains at the level of pixels and it is based on the preservation of the semantic content of the input image after the stylization. Thus, the semantic annotation of the original input image can be used to supervise the prediction of the network for the stylized image, as the semantics are preserved.

This type of pixel-level adaptation has been followed in several previous works [20, 32] which attempt to learn the stylization with a separate deep network. We argue that a light-weight shallow mapping g for the stylization is more flexible, as stylization can be performed on-the-fly during the data loading stage of training and does not introduce unnecessary additional complexity to the overall architecture. The availability of pairs of source and target images serves such a shallow stylization well, as one image can use the other image as the reference style, so the mapping g is not fixed for a given input image but has greater variability. More formally, we can write the stylized source image of our training batch from Sec. 3.1 which is computed with this regime as

$$I_{s\to t} = g(I_s, I_t) \tag{3}$$

and the respective stylized target image as

$$I_{t\to s} = g(I_t, I_s). \tag{4}$$

The stylization mapping g is the same in both cases, only that the order of its arguments is flipped, as the output always has the content of the first argument and the style of the second one. Such shallow stylizations have been proposed in the color transfer work of Reinhard et al. [26] and in FDA [43] and have been shown [43] to perform favorably for UDA compared to stylization learned jointly with semantic segmentation. Our method is agnostic to the exact mapping g that is used for stylization. We have used both FDA [43] and simple color transfer [26] in its implementation motivated by the compelling results of such shallow stylization approaches, especially in the normal-to-adverse UDA setting [31]. For the details of the simple color transfer method of Reinhard et al., we refer the reader to the original paper [26]. However, as FDA has a more complex formulation, we review it here shortly for completeness. FDA works with the discrete Fourier transform of the source and target images and copies the low-frequency Fourier amplitude of the reference style image to the input content image. More formally, FDA implements (3) as

$$I_{s\to t} = \mathcal{F}^{-1}([M \odot \mathcal{F}_A(I_t) + (1-M) \odot \mathcal{F}_A(I_s), \mathcal{F}_P(I_s)]), \tag{5}$$

where M is an ideal low-pass filter, $\mathcal{F}_A(\cdot)$ denotes the Fourier amplitude, $\mathcal{F}_P(\cdot)$ denotes the Fourier phase, and $\mathcal{F}^{-1}$ denotes the inverse discrete Fourier transform. $I_{t\to s}$ can be computed conversely based on (4).

Since $I_{s\to t}$ is rendered at the style of the target domain and is thus aligned to the latter, [43] proposes to modify the basic setup of (2) and substitute the original source image I_s with the stylized source image $I_{s\to t}$ in the cross-entropy loss associated with the source domain, where the styliza-

tion can be performed with any shallow mapping:

$$\mathcal{L}_{\text{FDA}} = \mathcal{L}_{\text{CE}}(F, I_{s\to t}, Y_s) + \mathcal{L}_{\text{CE}}(F, I_t, \hat{Y}_t). \quad (6)$$

3.3. Feature Invariance Loss

However, by only applying cross-entropy losses on the stylized source image $I_{s\to t}$ and the target image I_t, the optimization (6) proposed in [43] neglects the fact that *two* views are available for each input image thanks to stylization, one in the style of the source domain and the other in the style of the target domain. In particular, (6) only leverages the views that are characterized by the style of the target domain and neglects I_s and $I_{t\to s}$, which are characterized by the style of the source domain. Our key insight is that by using both views of the images—each view corresponding to a different domain—in the training, we can promote *invariance* of the features generated by the network across domains and thus better align the two domains at the level of features, which aids domain adaptation.

A straightforward way to attempt such an alignment is by adding cross-entropy losses on the additional views which are not included in (6), namely I_s and $I_{t\to s}$:

$$\begin{aligned}\mathcal{L}_{\text{CE,full}} = \mathcal{L}_{\text{CE}}(F, I_{s\to t}, Y_s) + \mathcal{L}_{\text{CE}}(F, I_s, Y_s) \\ + \mathcal{L}_{\text{CE}}(F, I_t, \hat{Y}_t) + \mathcal{L}_{\text{CE}}(F, I_{t\to s}, \hat{Y}_t). \quad (7)\end{aligned}$$

Since the labels used to supervise the predictions of the network for I_s and $I_{s\to t}$ (respectively I_t and $I_{t\to s}$) in (7) are the same, the two predictions are indirectly attracted to the same point, which is expected to promote consistency across domains.

Nevertheless, we argue that the shared semantic content between I_s and $I_{s\to t}$ (respectively I_t and $I_{t\to s}$) allows to impose an even stronger constraint on the semantic segmentation network F. More specifically, typical deep semantic segmentation networks consist of an encoder and a decoder. The bottleneck layer between the encoder and the decoder produces high-level features which should ideally be invariant to the specific style or visual condition of the input, allowing the decoder to focus on parsing these features into the output semantic classes and to not have to further abstract from the specific style of the input. Thus, we can minimize the difference of features produced by the semantic segmentation network F for views of the same scene under different styles, which is exactly the setting we have been examining. More formally, we can analyze F as a composition of an encoder ϕ and a decoder ω, $F = \omega \circ \phi$. For two input images I and I' of the same dimensions, the features generated by the encoder are $\phi(I), \phi(I') \in \mathbb{R}^{D\times M\times N}$. We define our feature invariance loss as

$$\mathcal{L}_{\text{inv}}(F, I, I') = \frac{1}{DMN}\|\phi(I) - \phi(I')\|_{\text{F}}^2, \quad (8)$$

where $\|\cdot\|_{\text{F}}$ is the Frobenius norm.

Coming back to our UDA setup, we propose to apply our feature invariance loss on the pairs of views $(I_s, I_{s\to t})$ and $(I_t, I_{t\to s})$ in order to align the features of the views from each pair. The two resulting feature invariance losses are combined with the cross-entropy losses of the basic setup of (2) in our final formulation of CISS as

$$\begin{aligned}\mathcal{L}_{\text{CISS}} = \mathcal{L}_{\text{CE}}(F, I_s, Y_s) + \mathcal{L}_{\text{CE}}(F, I_t, \hat{Y}_t) \\ + \lambda_s\mathcal{L}_{\text{inv}}(F, I_s, I_{s\to t}) + \lambda_t\mathcal{L}_{\text{inv}}(F, I_t, I_{t\to s}), \quad (9)\end{aligned}$$

where λ_s and λ_t are tunable hyperparameters. Note that we use cross-entropy losses only on the original images I_s and I_t, as the cross-entropy losses on the stylized images $I_{s\to t}$ and $I_{t\to s}$ which are used in (7) are redundant due to the inclusion of the feature invariance losses. In Sec. 4, we thoroughly ablate the final formulation in (9) and compare it to the basic formulation in (2) and the alternative formulations in (6) and (7), demonstrating the benefit of introducing feature invariance loss compared to training with the other formulations.

4. Experiments

4.1. Experimental Setup

Implementation details. The default implementation of CISS is based on HRDA [13]. Our semantic segmentation network comprises an MiT-B5 encoder from SegFormer [42] and a context-aware feature fusion decoder [12]. We also implement CISS with a DeepLabv2 [3] architecture involving a ResNet-101 backbone [9], in order to compare directly to several earlier UDA methods which use this architecture. For the default HRDA-based implementation, we follow the teacher-student self-training framework of DAFormer [12] with confidence-weighted pseudolabels, rare class sampling, and target data augmentation following DACS [34], and we use the AdamW optimizer [21] with a learning rate of 6×10^{-5} for the encoder and 6×10^{-4} for the decoder, a linear learning rate warm-up, and mini-batches of size $B = 2$. We follow the default configuration and parameters of HRDA regarding its multi-resolution setup. Unless otherwise stated, we use FDA [43] by default for stylization. Alternatively and only when explicitly stated, we use the color transfer of [26] for stylization. In the application of FDA stylization, we use $\beta = 0.01$ as the bandwidth parameter of the low-frequency band of the Fourier spectrum. We set the default values of the weights of the feature invariance losses in (9) for adaptation from Cityscapes to ACDC to $\lambda_s = 50$ and $\lambda_t = 20$ for the default HRDA-based implementation of CISS and to $\lambda_s = \lambda_t = 10$ for the alternative DeepLabv2-based implementation. For adaptation from Cityscapes to Dark Zurich, we set $\lambda_s = 100$ and $\lambda_t = 50$. We provide a study of these weights in Sec. 4.3.

Table 1. **Comparison of state-of-the-art unsupervised domain adaptation methods on Cityscapes→ACDC.** Cityscapes serves as the source domain and the entire ACDC including all four adverse conditions serves as the target domain. The first, second and third groups of rows present methods trained externally on Cityscapes→Dark Zurich, DeepLabv2-based UDA methods and SegFormer-based UDA methods, respectively. Results of DACS are taken from [2].

Method	road	sidew.	build.	wall	fence	pole	light	sign	veget.	terrain	sky	person	rider	car	truck	bus	train	motorc.	bicycle	mIoU
MGCDA [30]	76.0	49.4	72.0	11.3	21.7	39.5	52.0	54.9	73.7	24.7	88.6	54.1	27.2	78.2	30.9	41.9	58.2	31.1	44.4	48.9
GCMA [29]	79.7	48.7	71.5	21.6	29.9	42.5	56.7	57.7	75.8	39.5	**87.2**	57.4	29.7	80.6	44.9	46.2	62.0	37.2	46.5	53.4
AdaptSegNet [35]	69.4	34.0	52.8	13.5	18.0	4.3	14.9	9.7	64.0	23.1	38.2	38.6	20.1	59.3	35.6	30.6	53.9	19.8	33.9	33.4
BDL [20]	56.0	32.5	68.1	20.1	17.4	15.8	30.2	28.7	59.9	25.3	37.7	28.7	25.5	70.2	39.6	40.5	52.7	29.2	38.4	37.7
CLAN [22]	79.1	29.5	45.9	18.1	21.3	22.1	35.3	40.7	67.4	29.4	32.8	42.7	18.5	73.6	42.0	31.6	55.7	25.4	30.7	39.0
CRST [48]	51.7	24.4	67.8	13.3	9.7	30.2	38.2	34.1	58.0	25.2	76.8	39.9	17.1	65.4	3.7	6.6	39.6	11.8	8.6	32.8
FDA [43]	73.2	34.7	59.0	24.8	29.5	28.6	43.3	44.9	70.1	28.2	54.7	47.0	28.5	74.6	44.8	52.3	63.3	28.3	39.5	45.7
SIM [38]	53.8	6.8	75.5	11.6	22.3	11.7	23.4	25.7	66.1	8.3	80.6	41.8	24.8	49.7	38.6	21.0	41.8	25.1	29.6	34.6
MRNet [46]	72.2	8.2	36.4	13.7	18.5	20.4	38.7	45.4	70.2	35.7	5.0	47.8	19.1	73.6	42.1	36.0	47.4	17.7	37.4	36.1
DACS [34]	58.5	34.7	76.4	20.9	22.6	31.7	32.7	46.8	58.7	39.0	36.3	43.7	20.5	72.3	39.6	34.8	51.1	24.6	38.2	41.2
CISS-DeepLabv2	70.5	36.7	67.0	29.4	30.2	31.6	45.6	48.9	70.4	24.7	65.5	48.2	31.1	76.6	45.7	47.0	62.8	26.8	38.9	47.2
DAFormer [12]	58.4	51.3	84.0	42.7	35.1	50.7	30.0	57.0	74.8	52.8	51.3	58.2	32.6	82.7	58.3	54.9	82.4	44.1	50.7	55.4
SePiCo [41]	61.3	48.6	84.9	39.6	**40.3**	54.2	48.9	60.6	74.8	54.3	57.2	65.2	38.3	84.8	66.2	60.4	85.5	44.5	53.1	59.1
HRDA [13]	88.3	57.9	88.1	55.2	36.7	**56.3**	62.9	65.3	74.2	57.7	85.9	68.8	45.6	88.5	**76.4**	**82.4**	**87.7**	52.7	60.4	68.0
CISS (ours)	**91.9**	**69.3**	**89.3**	**57.0**	40.0	55.4	**67.2**	**67.2**	**75.2**	**59.6**	86.4	**69.7**	**47.2**	**89.0**	72.9	78.3	87.1	**55.7**	**61.8**	**69.5**

Datasets. In our experiments, we focus on the setting of domain adaptation and generalization from normal to adverse visual conditions, as our method is tailored for condition-level domain shifts that affect the appearance and texture of objects in the scene and not for structural-level shifts, as in the synthetic-to-real scenario. We use Cityscapes [5] as the labeled source-domain set in our experiments. Cityscapes is a large dataset of urban driving scenes, captured in several cities of central Europe under normal conditions and containing high-quality pixel-level semantic annotations for a set of 19 common classes in driving scenes. It consists of a training set with 2975 images, a validation set with 500 images, and a test set with 1525 images. When training UDA methods in our experiments, we sample source images only from the training set of Cityscapes. In addition, we use ACDC [31] and Dark Zurich [30] as unlabeled target-domain sets, which model the adverse-condition domain for normal-to-adverse UDA. ACDC consists of 4006 images of driving scenes distributed evenly among four common adverse conditions, i.e., night, fog, rain, and snow. Its training, validation and test set contain 1600, 406 and 2000 images respectively. Dark Zurich comprises 2617 nighttime images of driving scenes, which are split into 2416 training, 50 validation, and 151 test images. Both ACDC and Dark Zurich feature high-quality semantic annotations for the same set of 19 classes as Cityscapes. In our experiments, we use the training set of ACDC, resp. Dark Zurich, as the unlabeled target training set, evaluate on the validation set for ablations and hyperparameter studies, and evaluate only our final models against competing methods on the test set, which has withheld annotations and thus serves as a competitive public UDA benchmark. Finally, for models adapted to nighttime segmentation on Dark Zurich, we use BDD100K-night [30, 44] and Nighttime Driving [6] as target sets for generalization. BDD100K-night consists of 87 nighttime images with accurate segmentation labels and is a subset of the BDD100K segmentation dataset [44]. Nighttime Driving contains 50 nighttime images with coarsely annotated ground-truth.

4.2. Comparison to the State of the Art

We present the comparison of CISS to competing state-of-the-art UDA methods on Cityscapes→ACDC adaptation in Table 1. CISS significantly outperforms all competing methods, with a margin of 1.5% in the main mIoU metric from the second-best method. Moreover, our method achieves the best IoU in 13 out of the 19 individual classes, excelling in classes that are crucial for driving perception, such as road, sidewalk, traffic light, traffic sign, person, rider, and car. Focusing on the methods that use a DeepLabv2 architecture, CISS-DeepLabv2 also has the top performance among them, showing that the benefit of our method is general across different UDA architectures.

We provide a condition-specific comparison of CISS to competing unsupervised domain adaptation methods on the four adverse conditions of ACDC in Table 2. DANNet [39] and CuDA-Net [23] are specifically designed for night and fog respectively, so they only report results on those conditions. For the rest of the methods in Table 2, a single model is trained using the entire ACDC as the target set and is then evaluated separately on each condition. CISS performs favorably compared to other methods, both special-

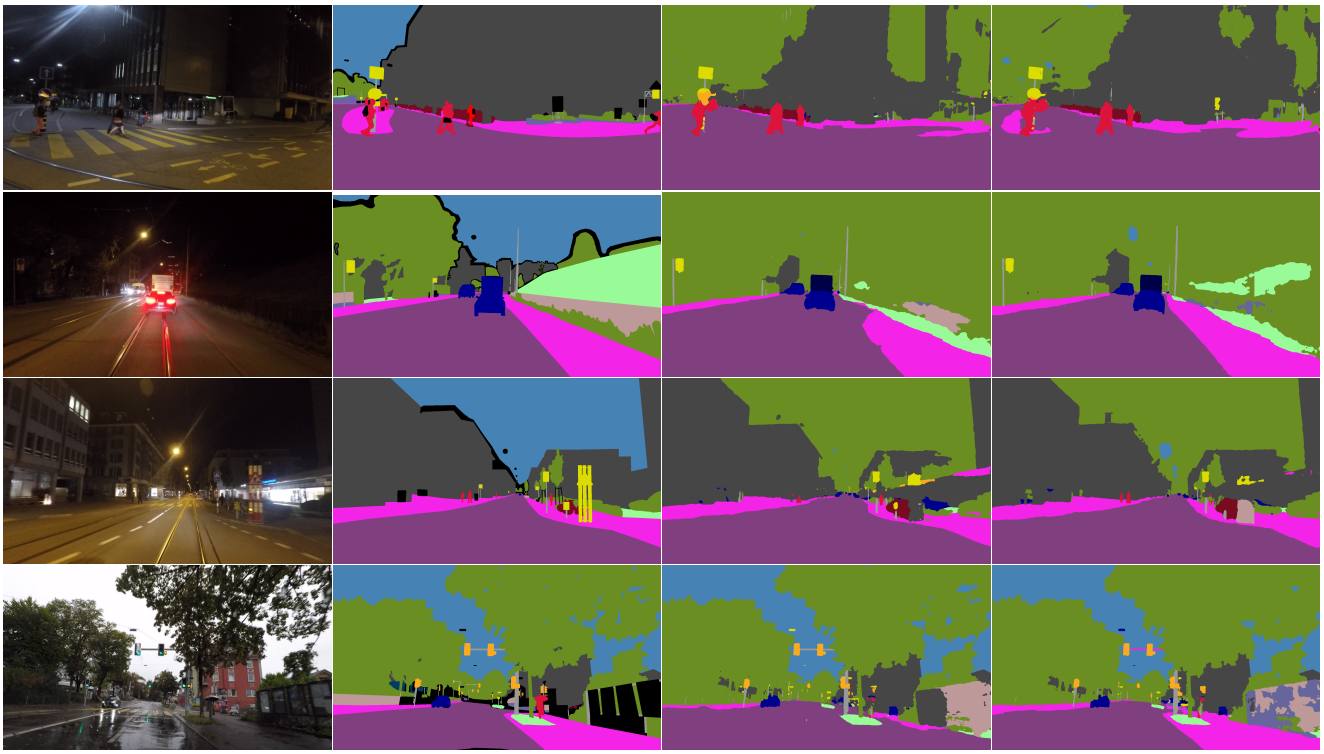

Figure 3. **Qualitative results on Cityscapes→ ACDC.** From left to right: ACDC image, ground-truth annotation, HRDA [13], and CISS. Best viewed on a screen and zoomed in.

Table 2. **Comparison of state-of-the-art unsupervised domain adaptation methods on Cityscapes→ACDC on individual conditions.** Training is performed on the entire Cityscapes and ACDC including all four conditions, while the single trained model of each method is evaluated separately on each condition, except for the first group of rows, where a single condition of ACDC is used both for training and evaluation. Results are reported using mIoU.

Method	Night	Fog	Rain	Snow
DANNet [39]	47.6	–	–	–
CuDA-Net [23]	–	55.6	–	–
GCMA [29]	42.9	52.4	58.0	53.8
MALL [25]	36.9	52.4	57.0	51.4
SePiCo [41]	50.5	58.5	66.1	57.9
HRDA [13]	53.1	**69.9**	73.6	69.5
CISS (ours)	**58.1**	68.8	**74.1**	**69.7**

ized and general ones. In particular, our method substantially improves upon the second-best method by 5.0% in mIoU on the challenging condition of night, which presents very large domain shifts from normal conditions, due to the much lower and more spatially-variant illumination compared to the source, daytime domain. These results place CISS in the first position of the public ACDC leaderboards[1] for semantic segmentation on the complete ACDC test set including all conditions as well as on the night, snow, and rain test sets among published unsupervised domain adaptation methods.

Qualitative comparisons of CISS to the highest-performing competing method on Cityscapes→ACDC, i.e. HRDA [13], are presented in Fig. 3, showing segmentation results on validation images of ACDC. On the top nighttime image, our method successfully segments both the traffic signs and most of the sidewalk, whereas HRDA mistakes one of the traffic signs for a traffic light and most of the sidewalk for road, which would be detrimental for the safety of the pedestrians standing on the sidewalk. On the nighttime image in the second row, CISS accurately segments most of the sidewalk on the right and also detects part of the terrain, even though the latter appears very dark. On the bottom rainy image, HRDA incorrectly segments a green reflection of a traffic light on the road as traffic light, while CISS correctly assigns this reflection to road and also segments the sidewalk on the right much more precisely.

In Table 3, we present the results of state-of-the-art SegFormer-based UDA methods on the challenging normal-to-adverse Cityscapes→Dark Zurich domain adaptation benchmark. Overall, CISS outperforms the other methods by a wide margin, improving by 3.1% mIoU over the second-best method, HRDA.

To further test the utility of CISS for condition-level adaptation, we compare it in Table 4 to state-of-the-art

[1] https://acdc.vision.ee.ethz.ch/benchmarks

Table 3. **Comparison of state-of-the-art unsupervised domain adaptation methods on Cityscapes→Dark Zurich.**

Method	road	sidew.	build.	wall	fence	pole	light	sign	veget.	terrain	sky	person	rider	car	truck	bus	train	motorc.	bicycle	mIoU
DAFormer [12]	**93.5**	65.5	73.3	39.4	19.2	53.3	44.1	44.0	59.5	34.5	66.6	53.4	52.7	82.1	52.7	9.5	89.3	50.5	38.5	53.8
SePiCo [41]	93.2	**68.1**	73.7	32.8	16.3	54.6	49.5	48.1	**74.2**	31.0	**86.3**	57.9	50.9	82.4	52.2	1.3	83.8	43.9	29.8	54.2
HRDA [13]	90.4	56.3	72.0	39.5	**19.5**	57.8	**52.7**	43.1	59.3	29.1	70.5	60.0	**58.6**	84.0	**75.5**	**11.2**	90.5	51.6	**40.9**	55.9
CISS (ours)	**93.5**	68.0	**80.9**	**47.5**	16.3	**59.8**	36.8	**55.2**	72.7	**38.0**	84.2	**61.1**	57.4	**86.3**	69.6	10.8	**90.8**	**53.3**	38.4	**59.0**

Table 4. **Comparison of state-of-the-art domain adaptation methods on generalization to BDD100K-night and Nighttime Driving.** All methods are trained on Cityscapes→Dark Zurich.

Method	BDD100K-night	Nighttime Driving
GCMA [29]	33.2	45.6
MGCDA [30]	34.9	49.4
DANNet [39]	27.2	47.7
DAFormer [12]	33.8	54.1
SePiCo [41]	40.6	56.9
HRDA [13]	40.2	57.7
CISS (ours)	**41.2**	**57.8**

Table 5. **Ablation study of CISS on Cityscapes→ACDC.** Evaluation is performed on the validation set of ACDC. "CE": cross-entropy loss, "Inv": feature invariance loss, "orig": original images from respective domain, "stylized": images from respective domain stylized with FDA. Mean and standard deviation across three runs are reported.

	Source			**Target**			mIoU
	CE orig	CE stylized	Inv	CE orig	CE stylized	Inv	
1	✓			✓			64.1±2.0
2		✓		✓			65.7±1.1
3	✓	✓		✓			65.1±0.7
4	✓		✓	✓			66.6±0.8
5	✓			✓		✓	66.9±0.5
6	✓		✓	✓	✓		65.7±1.2
7	✓		✓	✓		✓	**68.2**±0.4

domain adaptation methods on the challenging nighttime BDD100K-night and Nighttime Driving sets for generalization. In particular, all compared methods are trained for adaptation to nighttime using Dark Zurich [30] as their target domain. CISS outperforms all other methods, setting the new state of the art on both BDD100K-night and Nighttime Driving, and showing that our method adapts robustly to the target condition.

4.3. Ablation Studies

In Table 5, we conduct an ablation study of our method w.r.t. the various loss terms that are included in our overall loss $\mathcal{L}_{\text{CISS}}$ in (9) and the alternative loss terms that are included in the baseline formulations of (2), (6), and (7). The basic UDA formulation of (2), i.e., plain HRDA, corresponds to row 1. Switching to the FDA loss of (6) in row 2, i.e., pixel-level adaptation, improves upon the basic formulation. However, applying cross-entropy loss both for the original source images and their stylized versions (row 3), in the direction of (7), does not provide any gain over the FDA loss, evidencing that simultaneous output supervision on different views of images alone is not sufficient for aligning their features. On the contrary, applying the feature invariance loss on the source domain alone (row 4) improves upon the FDA setting of row 2, showing the utility of feature-level adaptation achieved with CISS on top of the pixel-level adaptation with FDA. In addition, the feature invariance loss applied solely on the target domain (row 5) also improves significantly upon the basic UDA setup of row 1. While using stylized target images for applying an additional cross-entropy loss on the target domain hurts performance (cf. rows 4 and 6), combining the two feature invariance losses from the source and the target domain in the complete formulation of CISS (9) (row 7) improves further compared to applying each of the two losses alone (rows 4 and 5), showing that the two losses synergize and achieve the best result.

Table 6. **Hyperparameter study of the weights of our feature invariance losses on Cityscapes→ACDC.** Evaluation is performed on the validation set of ACDC. Mean and standard deviation of mIoU across three runs are reported.

λ_s	50	100	200	500	1000
CISS-source	65.8±1.6	65.6±0.8	**66.6**±0.8	65.7±0.9	65.9±0.5
λ_t	20	50	100	200	500
CISS-target	66.7±0.6	66.6±1.6	**66.9**±0.5	66.1±0.7	65.2±0.6

Table 7. **Comparison of CISS using different stylization techniques for applying feature invariance loss in the target domain for Cityscapes→ACDC adaptation.** Evaluation is performed on the validation set of ACDC. We compare the default FDA [43] stylization and the stylization using the method by Reinhard et al. [26]. Mean and standard deviation across three runs are reported.

Invariance Loss	Mean IoU (%)
None	64.1±2.0
With FDA stylization ($\lambda_t = 100$)	66.9±0.5
With Reinhard stylization ($\lambda_t = 2$)	66.7±0.7

Invariance loss weights. We examine the influence of the value of the two hyperparameters of CISS, i.e., the weights

λ_s and λ_t, on performance in Table 6. In particular, we consider the ablated versions of CISS in which either of the two feature invariance losses is included, the source one (CISS-source) or the target one (CISS-target), and vary the respective weight. The best performance is obtained at $\lambda_s = 200$ for CISS-source and at $\lambda_t = 100$ for CISS-target, however, note that performance degrades gracefully as we move away from these values, implying that our method is fairly insensitive to the exact values of these hyperparameters.

Different stylization techniques. We test CISS in Table 7 with the color transfer technique in [26] for stylizing the input images, in order to verify its generality with regard to the stylization method that is used for imposing feature invariance. In particular, we consider the case where feature invariance is applied in the target domain and test CISS both with the default FDA stylization and with [26]. CISS improves significantly upon the baseline that does not use any feature invariance and it achieves similar performance with both stylization methods, which evidences the generality of CISS with regard to the stylization method that it employs.

5. Conclusion

We have presented CISS, a UDA method for semantic segmentation tailored for condition-level domain shifts. Our method promotes invariance of the features extracted by the semantic segmentation network to visual conditions, which are modeled through the style of the input, by penalizing the difference between features of the same image viewed under the styles of the source and the target domain. We have performed a thorough experimental evaluation of CISS and showed that it excels on normal-to-adverse adaptation from Cityscapes to ACDC and Cityscapes to Dark Zurich. Last but not least, our model which has been adapted to Dark Zurich generalizes very well to other unseen nighttime domains, i.e., BDD100K-night and Nighttime Driving, demonstrating that condition invariance makes it more robust to diverse inputs.

References

[1] Iñigo Alonso, Alberto Sabater, David Ferstl, Luis Montesano, and Ana C. Murillo. Semi-supervised semantic segmentation with pixel-level contrastive learning from a class-wise memory bank. In *Proceedings of the IEEE/CVF International Conference on Computer Vision (ICCV)*, 2021. 3

[2] David Bruggemann, Christos Sakaridis, Prune Truong, and Luc Van Gool. Refign: Align and refine for adaptation of semantic segmentation to adverse conditions. In *Proceedings of the IEEE/CVF Winter Conference on Applications of Computer Vision (WACV)*, 2023. 6

[3] Liang-Chieh Chen, George Papandreou, Iasonas Kokkinos, Kevin Murphy, and Alan L. Yuille. DeepLab: Semantic image segmentation with deep convolutional nets, atrous convolution, and fully connected CRFs. *IEEE Transactions on Pattern Analysis and Machine Intelligence*, 40(4):834–848, 2018. 5

[4] Yuhua Chen, Wen Li, and Luc Van Gool. ROAD: Reality oriented adaptation for semantic segmentation of urban scenes. In *The IEEE Conference on Computer Vision and Pattern Recognition (CVPR)*, 2018. 2

[5] Marius Cordts, Mohamed Omran, Sebastian Ramos, Timo Rehfeld, Markus Enzweiler, Rodrigo Benenson, Uwe Franke, Stefan Roth, and Bernt Schiele. The Cityscapes dataset for semantic urban scene understanding. In *The IEEE Conference on Computer Vision and Pattern Recognition (CVPR)*, 2016. 6

[6] Dengxin Dai and Luc Van Gool. Dark model adaptation: Semantic image segmentation from daytime to nighttime. In *2018 21st International Conference on Intelligent Transportation Systems (ITSC)*, pages 3819–3824. IEEE, 2018. 2, 6

[7] Geoff French, Samuli Laine, Timo Aila, Michal Mackiewicz, and Graham Finlayson. Semi-supervised semantic segmentation needs strong, varied perturbations. In *Proceedings of the British Machine Vision Conference (BMVC)*, 2020. 3

[8] Xiaoqing Guo, Jie Liu, Tongliang Liu, and Yixuan Yuan. SimT: Handling open-set noise for domain adaptive semantic segmentation. In *Proceedings of the IEEE/CVF Conference on Computer Vision and Pattern Recognition (CVPR)*, 2022. 2

[9] Kaiming He, Xiangyu Zhang, Shaoqing Ren, and Jian Sun. Deep residual learning for image recognition. In *The IEEE Conference on Computer Vision and Pattern Recognition (CVPR)*, June 2016. 5

[10] Judy Hoffman, Eric Tzeng, Taesung Park, Jun-Yan Zhu, Phillip Isola, Kate Saenko, Alexei Efros, and Trevor Darrell. CyCADA: Cycle-consistent adversarial domain adaptation. In *International Conference on Machine Learning*, 2018. 2

[11] Judy Hoffman, Dequan Wang, Fisher Yu, and Trevor Darrell. FCNs in the wild: Pixel-level adversarial and constraint-based adaptation. *arXiv e-prints*, abs/1612.02649, December 2016. 2

[12] Lukas Hoyer, Dengxin Dai, and Luc Van Gool. DAFormer: Improving network architectures and training strategies for domain-adaptive semantic segmentation. In *Proceedings of the IEEE/CVF Conference on Computer Vision and Pattern Recognition (CVPR)*, 2022. 3, 5, 6, 8, 13, 14

[13] Lukas Hoyer, Dengxin Dai, and Luc Van Gool. HRDA: Context-aware high-resolution domain-adaptive semantic segmentation. In *The European Conference on Computer Vision (ECCV)*, 2022. 1, 2, 3, 5, 6, 7, 8, 12, 13, 14, 15

[14] Zhengkai Jiang, Yuxi Li, Ceyuan Yang, Peng Gao, Yabiao Wang, Ying Tai, and Chengjie Wang. Prototypical contrast adaptation for domain adaptive semantic segmentation. In *European Conference on Computer Vision (ECCV)*, 2022. 3

[15] Myeongjin Kim and Hyeran Byun. Learning texture invariant representation for domain adaptation of semantic segmentation. In *IEEE/CVF Conference on Computer Vision and Pattern Recognition (CVPR)*, June 2020. 2

[16] Xin Lai, Zhuotao Tian, Xiaogang Xu, Yingcong Chen, Shu Liu, Hengshuang Zhao, Liwei Wang, and Jiaya Jia. DecoupleNet: Decoupled network for domain adaptive semantic segmentation. In *European Conference on Computer Vision (ECCV)*, 2022. 2

[17] Geon Lee, Chanho Eom, Wonkyung Lee, Hyekang Park, and Bumsub Ham. Bi-directional contrastive learning for domain adaptive semantic segmentation. In *European Conference on Computer Vision (ECCV)*, 2022. 3

[18] Sohyun Lee, Taeyoung Son, and Suha Kwak. FIFO: Learning fog-invariant features for foggy scene segmentation, 2022. 2

[19] Ruihuang Li, Shuai Li, Chenhang He, Yabin Zhang, Xu Jia, and Lei Zhang. Class-balanced pixel-level self-labeling for domain adaptive semantic segmentation. In *Proceedings of the IEEE/CVF Conference on Computer Vision and Pattern Recognition (CVPR)*, 2022. 2

[20] Yunsheng Li, Lu Yuan, and Nuno Vasconcelos. Bidirectional learning for domain adaptation of semantic segmentation. In *The IEEE Conference on Computer Vision and Pattern Recognition (CVPR)*, 2019. 1, 2, 4, 6, 13, 14

[21] Ilya Loshchilov and Frank Hutter. Decoupled weight decay regularization. In *ICLR*, 2018. 5

[22] Yawei Luo, Liang Zheng, Tao Guan, Junqing Yu, and Yi Yang. Taking a closer look at domain shift: Category-level adversaries for semantics consistent domain adaptation. In *The IEEE Conference on Computer Vision and Pattern Recognition (CVPR)*, 2019. 1, 2, 6, 13, 14

[23] Xianzheng Ma, Zhixiang Wang, Yacheng Zhan, Yinqiang Zheng, Zheng Wang, Dengxin Dai, and Chia-Wen Lin. Both style and fog matter: Cumulative domain adaptation for semantic foggy scene understanding. In *Proceedings of the IEEE/CVF Conference on Computer Vision and Pattern Recognition (CVPR)*, 2022. 6, 7, 13

[24] Luke Melas-Kyriazi and Arjun K. Manrai. PixMatch: Unsupervised domain adaptation via pixelwise consistency training. In *Proceedings of the IEEE/CVF Conference on Computer Vision and Pattern Recognition (CVPR)*, 2021. 3

[25] Nikhil Reddy, Abhinav Singhal, Abhishek Kumar, Mahsa Baktashmotlagh, and Chetan Arora. Master of all: Simultaneous generalization of urban-scene segmentation to all adverse weather conditions. In *European Conference on Computer Vision (ECCV)*, 2022. 7, 13, 14

[26] Erik Reinhard, Michael Adhikhmin, Bruce Gooch, and Peter Shirley. Color transfer between images. *IEEE Computer graphics and applications*, 21(5):34–41, 2001. 2, 4, 5, 8, 9

[27] Stephan R. Richter, Vibhav Vineet, Stefan Roth, and Vladlen Koltun. Playing for data: Ground truth from computer games. In *European Conference on Computer Vision*. Springer, 2016. 1

[28] German Ros, Laura Sellart, Joanna Materzynska, David Vazquez, and Antonio M. Lopez. The SYNTHIA dataset: A large collection of synthetic images for semantic segmentation of urban scenes. In *The IEEE Conference on Computer Vision and Pattern Recognition (CVPR)*, June 2016. 1

[29] Christos Sakaridis, Dengxin Dai, and Luc Van Gool. Guided curriculum model adaptation and uncertainty-aware evaluation for semantic nighttime image segmentation. In *The IEEE International Conference on Computer Vision (ICCV)*, 2019. 6, 7, 8, 12, 13, 14, 15

[30] Christos Sakaridis, Dengxin Dai, and Luc Van Gool. Map-guided curriculum domain adaptation and uncertainty-aware evaluation for semantic nighttime image segmentation. *IEEE Transactions on Pattern Analysis and Machine Intelligence*, 2020. 2, 6, 8, 12, 13, 14, 15

[31] Christos Sakaridis, Dengxin Dai, and Luc Van Gool. ACDC: The Adverse Conditions Dataset with Correspondences for semantic driving scene understanding. In *Proceedings of the IEEE/CVF International Conference on Computer Vision (ICCV)*, 2021. 1, 2, 4, 6

[32] Swami Sankaranarayanan, Yogesh Balaji, Arpit Jain, Ser Nam Lim, and Rama Chellappa. Learning from synthetic data: Addressing domain shift for semantic segmentation. In *IEEE Conference on Computer Vision and Pattern Recognition (CVPR)*, June 2018. 2, 4

[33] Kihyuk Sohn, David Berthelot, Nicholas Carlini, Zizhao Zhang, Han Zhang, Colin A. Raffel, Ekin Dogus Cubuk, Alexey Kurakin, and Chun-Liang Li. FixMatch: Simplifying semi-supervised learning with consistency and confidence. In *Advances in Neural Information Processing Systems*, 2020. 3

[34] Wilhelm Tranheden, Viktor Olsson, Juliano Pinto, and Lennart Svensson. DACS: Domain adaptation via cross-domain mixed sampling. In *Proceedings of the IEEE/CVF Winter Conference on Applications of Computer Vision (WACV)*, 2021. 1, 5, 6, 13, 14

[35] Yi-Hsuan Tsai, Wei-Chih Hung, Samuel Schulter, Kihyuk Sohn, Ming-Hsuan Yang, and Mammohan Chandraker. Learning to adapt structured output space for semantic segmentation. In *The IEEE Conference on Computer Vision and Pattern Recognition (CVPR)*, 2018. 1, 2, 6, 13, 14

[36] Yi-Hsuan Tsai, Kihyuk Sohn, Samuel Schulter, and Manmohan Chandraker. Domain adaptation for structured output via discriminative patch representations. In *IEEE/CVF International Conference on Computer Vision (ICCV)*, October 2019. 2

[37] Tuan-Hung Vu, Himalaya Jain, Maxime Bucher, Matthieu Cord, and Patrick Perez. ADVENT: Adversarial entropy minimization for domain adaptation in semantic segmentation. In *The IEEE Conference on Computer Vision and Pattern Recognition (CVPR)*, 2019. 1, 2

[38] Zhonghao Wang, Mo Yu, Yunchao Wei, Rogerio Feris, Jinjun Xiong, Wen-mei Hwu, Thomas S. Huang, and Honghui Shi. Differential treatment for stuff and things: A simple unsupervised domain adaptation method for semantic segmentation. In *IEEE/CVF Conference on Computer Vision and Pattern Recognition (CVPR)*, June 2020. 1, 2, 6, 13, 14

[39] Xinyi Wu, Zhenyao Wu, Hao Guo, Lili Ju, and Song Wang. DANNet: A one-stage domain adaption network for unsupervised nighttime semantic segmentation. In *IEEE/CVF Conference on Computer Vision and Pattern Recognition (CVPR)*, June 2021. 6, 7, 8, 12, 13, 14, 15

[40] Zhenyao Wu, Xinyi Wu, Xiaoping Zhang, Lili Ju, and Song Wang. SiamDoGe: Domain generalizable semantic segmentation using siamese network. In *European Conference on Computer Vision (ECCV)*, 2022. 3

[41] Binhui Xie, Shuang Li, Mingjia Li, Chi Harold Liu, Gao Huang, and Guoren Wang. SePiCo: Semantic-guided pixel contrast for domain adaptive semantic segmentation. *CoRR*, abs/2204.08808, 2022. 3, 6, 7, 8, 13, 14, 15

[42] Enze Xie, Wenhai Wang, Zhiding Yu, Anima Anandkumar, Jose M Alvarez, and Ping Luo. SegFormer: Simple and efficient design for semantic segmentation with transformers. In *Advances in Neural Information Processing Systems*, 2021. 5

[43] Yanchao Yang and Stefano Soatto. FDA: Fourier domain adaptation for semantic segmentation. In *IEEE/CVF Conference on Computer Vision and Pattern Recognition (CVPR)*, June 2020. 2, 3, 4, 5, 6, 8, 13, 14

[44] Fisher Yu, Haofeng Chen, Xin Wang, Wenqi Xian, Yingying Chen, Fangchen Liu, Vashisht Madhavan, and Trevor Darrell. BDD100K: A diverse driving dataset for heterogeneous multitask learning. In *IEEE/CVF Conference on Computer Vision and Pattern Recognition (CVPR)*, June 2020. 2, 6

[45] Yiheng Zhang, Zhaofan Qiu, Ting Yao, Dong Liu, and Tao Mei. Fully convolutional adaptation networks for semantic segmentation. In *The IEEE Conference on Computer Vision and Pattern Recognition (CVPR)*, 2018. 2

[46] Zhedong Zheng and Yi Yang. Rectifying pseudo label learning via uncertainty estimation for domain adaptive semantic segmentation. *International Journal of Computer Vision*, 2021. 1, 6, 13, 14

[47] Jun-Yan Zhu, Taesung Park, Phillip Isola, and Alexei A. Efros. Unpaired image-to-image translation using cycle-consistent adversarial networks. In *The IEEE International Conference on Computer Vision (ICCV)*, 2017. 2

[48] Yang Zou, Zhiding Yu, Xiaofeng Liu, B.V.K. Vijaya Kumar, and Jinsong Wang. Confidence regularized self-training. In *IEEE/CVF International Conference on Computer Vision (ICCV)*, October 2019. 1, 2, 6, 13, 14

[49] Yang Zou, Zhiding Yu, B.V.K. Vijaya Kumar, and Jinsong Wang. Unsupervised domain adaptation for semantic segmentation via class-balanced self-training. In *The European Conference on Computer Vision (ECCV)*, 2018. 1, 2

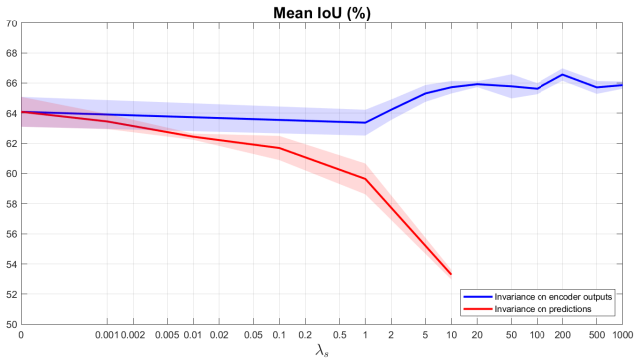

Figure 4. **Ablation of the point in the network where invariance is applied on Cityscapes→ACDC.** Evaluation is performed on the validation set of ACDC. The x-axis is logarithmic and shows the weight λ_s of the feature invariance loss, which is applied here only on the source domain. Averages and standard deviations are plotted over three runs for each configuration.

A. Ablation on the Point in the Network Where Invariance Is Applied

We justify the choice of applying feature invariance to the encoder outputs of the network in Fig. 4, which verifies our intuition that invariance on encoder outputs works better than on network outputs. In particular, using the feature invariance loss in the source domain, its application to encoder outputs improves significantly upon not using the invariance loss at all, while its application to network outputs, i.e. predictions, deteriorates performance compared to not applying feature invariance at all.

B. Detailed Class-Level Quantitative Results on Individual Conditions of ACDC

In Tables 8, 9, 10, and 11, we provide detailed class-level IoU results on the condition-specific splits of the test set of ACDC for all methods which are presented in Tables 1 and 2 of the main paper.

CISS dominates the challenging nighttime benchmark of ACDC (cf. Table 8), scoring 5.0% higher on mean IoU than the second-best method and delivering substantial improvements in IoU on several central driving-related classes over the respective second-best method, such as on sidewalk (9.7%), traffic light (6.8%), traffic sign (7.6%), motorcycle (7.2%), and bicycle (4.3%). CISS achieves the best IoU score on 14 out of the 19 classes and is significantly outperformed only on two classes, namely vegetation and sky, and in those cases only by methods trained specifically on nighttime sets and using weak supervision [29, 30, 39].

Moreover, CISS achieves the best performance on the rain benchmark of ACDC (cf. Table 10). It outperforms the second-best method on this benchmark, HRDA [13], consistently on 13 out of the 19 classes, it is on a par with the latter on 2 classes, and it is slightly outperformed by the latter on classes with large instances (truck, bus, train), which only appear rarely in the scenes of ACDC.

CISS is also the top-performing method on the snow benchmark of ACDC (cf. Table 11). Even though it outperforms the second-best method, HRDA [13], only slightly in mean IoU, it achieves significant improvements over the latter on driving-related classes which exhibit large appearance shifts with respect to the source, normal-condition domain of Cityscapes due to snow cover on the ground, namely road and sidewalk.

Finally, although CISS is slightly outperformed by HRDA [13] in mean IoU on the fog benchmark of ACDC (cf. Table 9), the two methods are on a par with regard to class-level IoU scores. In particular, CISS outperforms HRDA on 9 classes, HRDA outperforms CISS on 9 classes, and the two methods obtain equal IoU scores on one class. CISS is better on several safety-critical classes, such as road, sidewalk, person, and rider, and the higher mean IoU score of HRDA is largely due to the large difference in the IoUs of the two methods on bus, which is a very rare class in ACDC.

C. Detailed Class-Level Quantitative Results on Generalization on BDD100K-night and Nighttime Driving

In Tables 12 and 13, we provide detailed class-level IoU results on the generalization performance of models adapted from Cityscapes to Dark Zurich on BDD100K-night and Nighttime Driving, respectively. CISS is consistently among the two top-performing methods on 7 out of the 8 dynamic classes on BDD100K-night and scores the top mean IoU result among competing state-of-the-art methods in this generalization experiment. Moreover, CISS achieves the best generalization performance on Nighttime Driving among state-of-the-art domain adaptation approaches. Note that despite the fact that CISS is only slightly better in terms of mean IoU performance on Nighttime Driving than the second-best method, HRDA, a head-to-head class-level comparison of the two methods reveals that CISS outperforms HRDA in 15 out of the 19 classes (in most of which significantly) and is outperformed only in 2, while the two methods are on a par in 2 classes. HRDA is favored by the fact that it has much higher performance on the truck class, which however is very rare in Nighttime Driving.

Table 8. **Comparison of state-of-the-art unsupervised domain adaptation methods on Cityscapes→ACDC for nighttime.** The first, second, third and fourth groups of rows present methods trained externally on Cityscapes→Dark Zurich, DeepLabv2-based UDA methods, a DeepLabv3+-based UDA method, and SegFormer-based UDA methods, respectively.

Method	road	sidew.	build.	wall	fence	pole	light	sign	veget.	terrain	sky	person	rider	car	truck	bus	train	motorc.	bicycle	mIoU
GCMA [29]	78.6	45.9	58.5	17.7	18.6	37.5	43.6	43.5	58.7	39.2	22.4	57.9	29.9	72.1	21.5	56.2	41.8	35.7	35.4	42.9
MGCDA [30]	74.5	52.5	69.4	7.7	10.8	38.4	40.2	43.3	61.5	36.3	37.6	55.3	25.6	71.2	10.9	46.4	32.6	27.3	33.8	40.8
DANNet [39]	90.7	61.1	75.5	35.9	**28.8**	26.6	31.4	30.6	**70.8**	39.4	**78.7**	49.9	28.8	65.9	24.7	44.1	61.1	25.9	34.5	47.6
AdaptSegNet [35]	84.9	39.9	66.8	17.2	17.7	13.4	17.6	16.4	39.6	16.1	5.7	42.8	21.4	44.8	11.9	13.0	39.1	27.5	28.4	29.7
BDL [20]	87.1	49.6	68.8	20.2	17.5	16.7	19.9	24.1	39.1	23.7	0.2	42.0	20.4	63.7	18.0	27.0	45.6	27.8	31.3	33.8
CLAN [22]	82.3	28.8	65.9	15.1	9.3	22.1	16.1	26.5	39.2	23.4	0.4	45.9	25.4	63.6	9.5	24.2	39.8	31.5	31.1	31.6
CRST [48]	43.9	10.0	57.3	10.0	5.1	29.3	27.0	18.6	6.9	8.2	0.3	36.9	17.9	48.5	4.9	1.8	29.4	7.3	8.8	19.6
FDA [43]	82.7	39.4	57.0	14.7	7.6	26.1	37.8	30.5	53.2	14.0	15.3	48.0	28.8	62.6	26.6	47.5	51.5	27.0	35.0	37.1
SIM [38]	87.0	48.4	42.1	6.3	8.3	15.8	8.4	17.6	21.7	22.8	0.1	39.3	22.1	60.3	8.7	18.2	42.3	30.1	32.9	28.0
MRNet [46]	83.6	36.3	65.6	8.1	8.2	21.5	30.0	23.7	39.4	24.2	0.0	44.1	26.0	64.9	0.8	3.6	7.6	10.3	31.8	27.9
DACS [34]	84.8	52.5	64.8	17.5	16.0	30.5	25.1	33.9	38.4	10.7	2.7	40.7	21.2	63.9	16.4	36.6	45.4	19.5	23.4	33.9
MALL [25]	78.9	26.8	62.2	25.3	19.9	32.3	32.6	31.4	49.9	27.9	13.5	47.3	19.6	61.0	19.2	35.4	56.0	29.7	31.4	36.9
DAFormer [12]	92.3	64.6	70.1	28.7	18.5	45.8	11.3	41.5	42.7	41.9	0.0	55.4	29.8	74.3	40.3	45.8	81.3	39.4	47.0	45.8
SePiCo [41]	89.9	56.8	75.6	35.3	28.4	49.5	24.7	50.1	43.4	44.5	4.8	61.1	34.1	77.3	62.0	52.9	79.5	41.2	48.3	50.5
HRDA [13]	87.2	46.9	79.1	46.2	18.0	51.4	41.0	48.5	41.8	46.7	0.0	63.2	36.9	81.0	**65.2**	**77.7**	83.6	46.0	49.0	53.1
CISS (ours)	**94.7**	**74.3**	**81.3**	**48.1**	28.0	**52.0**	**50.4**	**57.7**	43.1	**53.3**	2.4	**65.5**	**38.0**	**83.9**	63.0	75.8	**86.6**	**53.2**	**53.3**	**58.1**

Table 9. **Comparison of state-of-the-art unsupervised domain adaptation methods on Cityscapes→ACDC for fog.** The first, second, third, fourth and fifth groups of rows present methods trained externally on Cityscapes→Dark Zurich, a method trained externally on Cityscapes→Foggy Zurich, DeepLabv2-based UDA methods, a DeepLabv3+-based UDA method, and SegFormer-based UDA methods, respectively.

Method	road	sidew.	build.	wall	fence	pole	light	sign	veget.	terrain	sky	person	rider	car	truck	bus	train	motorc.	bicycle	mIoU
MGCDA [30]	71.7	47.3	65.7	18.2	15.3	34.4	48.6	59.9	64.9	24.7	95.4	44.8	23.8	73.3	36.1	45.4	63.9	23.9	15.4	45.9
GCMA [29]	80.8	53.5	70.1	29.2	20.7	38.4	53.0	60.9	70.2	46.5	95.4	44.2	38.0	76.6	52.4	49.7	56.8	41.0	17.6	52.4
CuDA-Net [23]	83.2	45.9	81.7	35.5	22.7	40.7	55.5	55.6	81.1	63.8	95.6	45.2	24.9	78.7	41.1	48.3	77.8	52.0	27.1	55.6
AdaptSegNet [35]	35.4	45.9	35.4	25.6	17.5	9.0	32.5	23.1	70.5	47.4	11.6	22.3	28.2	44.4	43.9	35.0	46.0	15.6	15.0	31.8
BDL [20]	36.9	37.8	47.0	28.2	21.6	13.7	37.2	34.5	67.2	49.4	27.6	29.1	51.3	58.5	49.4	51.8	30.3	21.4	22.5	37.7
CLAN [22]	48.8	41.3	29.6	27.2	21.0	16.1	41.1	39.6	67.7	50.2	15.4	36.2	30.8	72.2	52.2	54.4	47.2	27.1	22.6	39.0
CRST [48]	59.7	29.6	70.9	11.3	11.4	29.9	41.4	38.6	61.7	31.6	96.6	36.0	7.9	62.4	19.7	4.6	49.4	9.0	7.6	35.8
FDA [43]	68.8	37.3	27.1	27.6	19.8	21.6	37.5	43.3	74.9	43.7	33.1	35.0	21.5	65.7	44.6	45.3	47.1	41.5	15.8	39.5
SIM [38]	76.7	43.1	23.5	23.6	17.9	10.9	32.1	15.3	70.4	50.5	21.4	34.8	44.3	58.4	50.5	55.2	34.7	23.0	8.8	36.6
MRNet [46]	78.6	26.1	19.6	29.0	13.5	12.0	41.9	49.0	78.2	59.0	6.6	39.8	26.1	72.5	44.8	37.9	59.6	19.1	24.1	38.8
DACS [34]	34.9	51.8	79.0	22.8	24.8	22.9	20.0	46.6	50.5	50.8	19.7	38.2	25.9	69.5	44.1	48.5	29.9	28.8	16.0	38.1
MALL [25]	63.7	54.3	79.8	34.8	27.4	37.9	49.1	52.6	74.9	59.6	92.9	40.2	39.0	75.4	53.0	36.4	76.4	26.8	21.5	52.4
DAFormer [12]	38.9	42.4	86.8	52.5	26.8	46.7	45.6	57.3	86.4	64.7	56.5	37.6	53.3	76.2	60.8	32.4	64.0	52.1	29.6	53.2
SePiCo [41]	42.6	51.5	87.6	51.2	**31.2**	**52.4**	51.0	59.0	85.3	65.9	61.3	51.4	62.2	78.0	64.5	42.3	83.5	58.0	32.6	58.5
HRDA [13]	93.0	73.5	89.1	**56.4**	27.3	51.2	**62.2**	**69.5**	86.5	70.3	**98.0**	53.4	61.9	**85.6**	**77.1**	**88.3**	**84.9**	**64.1**	36.6	**69.9**
CISS (ours)	**94.0**	**76.2**	**89.9**	55.3	29.1	49.3	61.4	66.0	**87.0**	**71.8**	**98.0**	**54.2**	**63.5**	83.8	75.8	62.6	84.2	61.8	**42.3**	68.7

Table 10. **Comparison of state-of-the-art unsupervised domain adaptation methods on Cityscapes→ACDC for rain.** The first, second, third and fourth groups of rows present methods trained externally on Cityscapes→Dark Zurich, DeepLabv2-based UDA methods, a DeepLabv3+-based UDA method, and SegFormer-based UDA methods, respectively.

Method	road	sidew.	build.	wall	fence	pole	light	sign	veget.	terrain	sky	person	rider	car	truck	bus	train	motorc.	bicycle	mIoU
GCMA [29]	81.1	48.0	84.8	25.0	37.3	49.8	66.5	66.2	92.1	43.5	97.6	54.5	20.4	85.5	47.3	34.6	71.3	40.3	56.7	58.0
MGCDA [30]	80.5	46.5	79.9	16.0	28.8	44.9	60.0	61.5	90.3	44.8	97.1	51.1	23.1	82.3	33.4	30.2	69.1	36.5	53.8	54.2
AdaptSegNet [35]	81.2	43.2	83.3	27.3	31.4	23.0	41.4	40.5	87.2	35.0	93.1	40.2	15.5	73.9	45.7	34.9	57.0	27.1	49.1	49.0
BDL [20]	79.1	39.0	82.8	30.0	34.5	28.1	40.1	47.3	87.0	28.7	91.8	40.6	17.8	74.6	46.3	36.7	60.4	33.2	46.3	49.7
CLAN [22]	77.5	40.0	46.8	24.9	30.3	28.1	37.7	48.3	83.8	37.0	6.6	45.7	17.4	79.7	43.7	42.9	63.7	35.0	46.1	44.0
CRST [48]	58.8	26.4	77.1	20.0	12.1	32.8	45.3	41.7	78.6	38.4	95.7	40.5	12.8	74.7	25.6	5.5	51.8	23.7	10.9	40.6
FDA [43]	76.6	45.0	82.9	37.0	35.6	34.8	49.8	52.0	88.7	37.8	88.8	43.6	17.4	76.8	46.5	53.6	64.8	34.5	45.5	53.3
SIM [38]	76.6	29.6	85.7	20.4	28.7	21.3	37.4	34.2	87.3	34.8	94.0	29.4	16.6	73.2	46.1	22.3	46.2	21.8	39.3	44.5
MRNet [46]	70.5	9.9	46.5	35.6	36.1	36.5	56.4	56.2	90.2	41.3	4.3	53.0	23.5	81.6	39.3	26.7	57.8	43.6	54.5	45.4
DACS [34]	69.3	41.8	84.3	30.1	20.6	38.4	38.3	54.8	83.5	38.9	82.8	41.5	14.6	76.3	47.4	30.7	53.7	30.4	49.6	48.8
MALL [25]	75.9	38.1	87.6	35.9	38.6	45.9	60.7	60.1	88.8	38.7	96.6	48.9	14.2	84.8	56.4	63.8	71.7	27.7	47.8	57.0
DAFormer [12]	73.1	46.7	92.2	55.9	40.5	54.9	65.6	64.9	93.1	40.8	89.8	58.5	20.6	86.1	63.5	66.4	83.0	46.6	53.4	62.9
SePiCo [41]	80.1	47.3	90.1	48.9	48.2	57.0	70.4	66.5	93.2	43.2	93.8	67.3	26.4	89.0	68.1	71.5	88.8	49.6	57.0	66.1
HRDA [13]	**92.4**	73.6	93.8	67.0	46.3	**63.0**	74.5	74.2	93.7	46.1	97.6	69.4	32.5	91.7	**79.9**	**90.5**	**89.0**	57.8	**66.0**	73.6
CISS (ours)	**92.4**	**74.2**	**94.8**	**70.1**	**48.7**	61.0	**74.7**	**74.4**	**94.0**	**48.0**	**98.3**	**69.9**	**37.7**	**92.1**	74.7	89.8	88.0	**59.0**	**66.0**	**74.1**

Table 11. **Comparison of state-of-the-art unsupervised domain adaptation methods on Cityscapes→ACDC for snow.** The first, second, third and fourth groups of rows present methods trained externally on Cityscapes→Dark Zurich, DeepLabv2-based UDA methods, a DeepLabv3+-based UDA method, and SegFormer-based UDA methods, respectively.

Method	road	sidew.	build.	wall	fence	pole	light	sign	veget.	terrain	sky	person	rider	car	truck	bus	train	motorc.	bicycle	mIoU
GCMA [29]	79.7	49.5	75.3	17.5	37.9	43.2	59.0	61.9	78.8	2.2	95.5	62.5	33.6	83.2	42.5	43.4	72.1	32.2	51.1	53.7
MGCDA [30]	80.1	49.5	70.2	6.1	27.8	39.6	55.4	58.0	76.0	0.3	95.5	57.5	35.7	81.0	28.6	48.9	70.3	27.8	50.5	50.5
AdaptSegNet [35]	51.3	32.5	47.3	21.5	31.5	13.2	37.8	23.2	76.0	2.6	4.5	49.9	23.1	68.7	38.3	31.8	51.5	21.7	45.0	35.3
BDL [20]	42.3	36.4	60.2	15.7	30.4	15.1	41.4	30.4	71.3	1.7	11.2	46.8	27.8	57.7	38.6	34.1	59.2	28.1	43.7	36.4
CLAN [22]	71.8	26.0	37.3	12.5	27.0	21.1	32.0	41.1	78.5	1.9	0.9	50.9	23.9	82.4	43.2	39.5	61.6	25.2	39.4	37.7
CRST [48]	63.5	38.2	66.8	12.8	9.2	29.0	44.8	40.3	68.5	0.8	65.1	44.6	23.8	70.0	1.2	19.0	39.1	11.4	6.0	34.4
FDA [43]	74.6	30.9	56.1	20.5	34.8	28.7	53.9	47.8	80.5	1.1	55.9	53.1	37.9	79.7	40.5	51.9	67.4	34.3	41.8	46.9
SIM [38]	72.1	26.7	39.4	13.3	29.5	15.3	26.4	17.9	76.4	4.8	5.1	45.9	32.0	76.2	29.8	26.6	48.3	23.2	24.2	33.3
MRNet [46]	67.7	3.5	36.8	8.3	24.8	18.0	52.6	55.4	82.4	0.5	0.1	62.2	30.2	79.2	32.1	59.3	58.4	29.1	35.8	38.7
DACS [34]	52.4	13.7	77.7	14.2	24.7	33.2	40.3	50.6	78.8	0.8	34.2	51.7	22.2	75.0	30.8	30.6	58.4	19.8	43.9	39.6
MALL [25]	78.2	40.9	78.8	19.1	36.6	39.7	60.9	51.6	80.9	**6.8**	90.5	54.8	28.1	82.9	40.3	58.6	68.4	13.4	46.6	51.4
DAFormer [12]	38.1	41.3	88.3	42.1	47.2	54.2	71.1	64.2	91.2	4.5	32.8	66.0	36.4	88.0	54.4	71.3	84.5	46.0	54.8	56.7
SePiCo [41]	40.5	33.7	87.1	29.2	**50.0**	57.6	76.1	66.1	90.4	4.2	42.8	71.9	41.5	89.3	66.4	69.7	88.6	37.2	57.8	57.9
HRDA [13]	82.5	45.5	90.4	55.3	49.9	**58.9**	**77.7**	**71.9**	91.3	6.0	96.2	**79.6**	**62.8**	**92.0**	**73.8**	73.1	**90.4**	**52.0**	70.7	69.5
CISS (ours)	**84.0**	**50.7**	**91.0**	**58.0**	49.9	57.7	77.3	70.7	**91.4**	4.8	**96.8**	78.6	60.9	91.5	70.8	**79.2**	87.1	**52.0**	**71.2**	**69.7**

Table 12. **Comparison of state-of-the-art domain adaptation methods on generalization to BDD100K-night.** All methods are trained on Cityscapes→Dark Zurich. Best results in bold, second-best underlined.

Method	road	sidew.	build.	wall	fence	pole	light	sign	veget.	terrain	sky	person	rider	car	truck	bus	train	motorc.	bicycle	mIoU
GCMA [29]	85.8	48.1	64.1	1.4	16.3	30.4	**23.7**	34.9	43.1	6.8	5.9	65.4	**76.8**	78.8	15.3	29.8	0.0	0.0	3.8	33.2
MGCDA [30]	83.9	45.8	74.1	0.4	17.0	30.4	23.6	33.8	42.1	10.8	49.9	65.7	65.9	79.7	10.3	26.5	0.0	0.0	3.7	34.9
DANNet [39]	74.1	39.9	68.3	2.6	6.1	21.3	10.6	30.6	36.3	13.4	51.8	56.0	18.7	66.6	17.6	3.0	0.0	0.0	0.8	27.2
SePiCo [41]	**87.3**	48.3	80.2	3.3	12.2	**37.9**	20.1	**51.4**	**47.6**	**20.5**	65.5	67.6	67.1	**83.7**	29.9	46.3	0.0	0.0	1.9	40.6
HRDA [13]	84.8	**49.6**	77.0	4.5	**26.9**	35.7	21.7	47.3	35.4	12.3	60.4	66.9	27.6	81.4	**53.1**	**65.2**	0.0	0.0	**13.9**	40.2
CISS (ours)	85.1	44.8	**80.5**	**6.3**	25.7	37.2	20.9	45.6	42.7	12.5	**69.6**	**69.7**	74.1	83.5	47.8	23.8	0.0	0.0	13.3	**41.2**

Table 13. **Comparison of state-of-the-art domain adaptation methods on generalization to Nighttime Driving.** All methods are trained on Cityscapes→Dark Zurich.

Method	road	sidew.	build.	wall	fence	pole	light	sign	veget.	terrain	sky	person	rider	car	truck	bus	train	motorc.	bicycle	mIoU
GCMA [29]	86.0	47.0	82.2	10.7	0.0	49.4	69.5	72.1	69.0	0.0	20.3	65.1	**36.0**	71.1	0.0	75.8	69.8	0.0	42.9	45.6
MGCDA [30]	87.9	57.3	83.8	6.8	0.0	48.5	70.3	77.5	65.9	0.0	**66.2**	64.8	29.1	75.9	0.0	87.0	76.2	0.0	42.1	49.4
DANNet [39]	90.1	68.1	88.2	48.9	0.0	35.1	59.2	71.6	59.7	0.0	47.0	60.4	31.2	72.3	8.6	55.6	72.0	0.0	37.7	47.7
SePiCo [41]	**93.0**	**73.7**	**90.5**	54.8	**0.1**	67.5	80.5	82.2	**67.2**	0.0	58.5	62.2	**36.0**	75.0	18.3	94.6	92.8	0.0	34.5	56.9
HRDA [13]	87.6	52.6	85.7	70.3	0.0	69.0	78.7	82.2	46.3	0.0	44.4	**67.0**	34.6	76.2	**69.8**	93.4	93.1	0.0	46.2	57.7
CISS (ours)	**93.0**	73.6	89.8	**75.0**	**0.1**	**70.4**	**83.2**	**86.0**	59.2	0.0	54.4	64.1	35.0	**76.9**	0.0	**96.1**	**93.9**	0.0	**48.2**	**57.8**